

HITTITE JOURNAL OF SCIENCE AND ENGINEERING

e-ISSN: 2148-4171
Volume: 11 • Number: 3
September 2024

Assessment of Human Sperm Kinematic Parameters Using Computer-Assisted Semen Analysis

Nazlı Irmak Karaark  | Huseyin Kurtuldu* 

Başkent University, Department of Biomedical Engineering, 06790, Ankara, Türkiye

Corresponding Author

Huseyin Kurtuldu

E-mail: hkurtuldu@baskent.edu.tr Phone: +90 541 571 3194

RORID: <https://ror.org/02v9bqx10>

Article Information

Article Type: Research Article

Doi: <https://doi.org/10.17350/HJSE19030000340>

Received: 09.08.2022

Accepted: 29.08.2024

Published: 30.09.2024

Cite As

Karaark, N. I. & Kurtuldu, H. Assessment of Human Sperm Kinematic Parameters Using Computer-Assisted Semen Analysis. Hittite J Sci Eng. 2024;11(3):131-137.

Peer Review: Evaluated by independent reviewers working in at least two different institutions appointed by the field editor.

Ethical Statement: Not available.

Plagiarism Checks: Yes - iThenticate

Conflict of Interest: The author declares that there is no conflicts of interest concerning the content of this article

CRedit AUTHOR STATEMENT

Huseyin Kurtuldu: Conception, Design, Supervision, Providing, Materials, Data Collection or Processing, Analysis or Interpretation, Article Writing, Critical Review. **Nazlı Irmak Karaark:** Conception, Design, Supervision, Materials, Data Collection or Processing, Analysis or Interpretation, Literature Review, Article Writing, Critical Review.

Copyright & License: Authors publishing with the journal retain the copyright of their work licensed under CC BY-NC 4.

Assessment of Human Sperm Kinematic Parameters Using Computer-Assisted Semen Analysis

Nazlı Irmak Karaark | Huseyin Kurtuldu*

Başkent University, Department of Biomedical Engineering, 06790, Ankara, Türkiye

Abstract

Infertility affects approximately 15% of couples trying to conceive, as reported by the World Health Organization. It is diagnosed when conception does not occur despite unprotected intercourse over the course of at least one year. The spermogram test is a fundamental tool for identifying whether infertility originates from the male or female partner. Traditionally, sperm analysis is performed manually in reproductive clinics and laboratories, which may lead to variability in results due to subjective technician evaluations. Recent advancements have introduced computer-assisted systems with image processing capabilities to enhance sperm quality analysis. This study presents a novel computer-assisted sperm analysis (CASA) system designed to evaluate sperm motility through digital micrographs, utilizing 14 distinct kinematic parameters. The algorithms and parameters developed offer a quantitative approach to characterizing infertility.

Keywords: CASA, sperm analysis, kinematics, infertility, spermogram, semen

INTRODUCTION

Infertility is defined as the inability of couples to conceive after one year of unprotected intercourse [1]. Factors such as poor diet, stress, insomnia, smoking, and alcohol consumption can impair reproductive health, contributing to infertility. According to the World Health Organization (WHO), approximately 15% of couples seeking to conceive are affected by infertility [2]. With male reproductive issues accounting for about 50% of infertility cases [1], assessing male reproductive health is crucial in infertility diagnostics. Basic indicators of male fertility include the percentage of motile sperm and their velocity. Conventional sperm analysis, performed microscopically in clinical settings, often suffers from variability due to subjective evaluation [3]. Consequently, there is a need for fully automated systems that provide objective, standardized results.

Sperm imaging and motility studies have evolved over the past 300 years. Recent advancements focus on high-accuracy imaging techniques to improve treatment methods for reproductive disorders. The development of computer-assisted sperm analysis (CASA) began in the 1950s, enhancing classical microscopic imaging techniques. The introduction of phase contrast microscopy in andrology studies allowed better detection of sperm viability [4]. Automated sperm analysis methods date back to the early 1970s [4], with Katz et al. [5] pioneering the first CASA system in 1985, which assessed sperm motility from sequential microscopic images.

Abbiramy et al. [6] developed an algorithm in 2010 that could detect, count, and track sperm cells in video streams, achieving a 93% accuracy in tracking. Leung et al. [7] introduced algorithms to monitor sperm tail movement, improving Euclidean distance calculations. Ravanfar and Moradi [8] utilized Watershed segmentation and particle filter algorithms to address challenges in sperm tracking due to their similar size and shape. Di Caprio et al. [9] analyzed sperm motility by solving focal amplitude and phase maps from holographic images. Elsayed et al. [10] enhanced CASA systems in 2015 for better sperm detection in microfluidic systems using low-frame-rate cameras. Urbano et al. [11] employed the joint probabilistic data association filter in 2016 to simultaneously detect sperm movement and measure parameters without sample dilution. Boumazza and Loukil [12] developed an algorithm that enhances sperm analysis

by improving image quality and using hybrid segmentation techniques. Their method shows promising results for measuring sperm concentration and motility compared to traditional methods. Hernández-Ferrándiz, Pantrigo, and Cabido [13] introduced a method using synthetic semen samples to address the lack of labeled data in sperm analysis. Their approach demonstrates that models trained on synthetic data can be effectively applied to real images without additional fine-tuning.

This study introduces a CASA system incorporating sperm detection and tracking algorithms to provide quantitative measurements of human sperm kinematic parameters. The system was tested using samples from an 18-year-old subject, enabling numerical evaluation of male infertility and comparison with WHO and other institutional reference values.

MATERIAL AND METHODS

The study, approved by the Ankara City Hospital No. 2 Clinical Research Ethics Committee (Protocol No. E2-21-930) on October 13, 2021, utilized a sample obtained from the Andrology-Urology Clinic of Ankara City Hospital. The sample, from an 18-year-old subject referred to as Subject A, was a gray opaque, homogeneously distributed fluid with a volume of 3 ml and a pH of 7.5.

A 50 μm thick double-sided tape was placed between a microscope slide and coverslip, allowing sperm cells to move freely within a 50 μm depth. Sperm images were captured using a 2-megapixel camera mounted on an Olympus CX21 microscope at 10X magnification [14], covering a measurement area of 165.054 μm^2 and a volume of 8.252.749 μm^3 . Four series of images were captured at three-minute intervals, with each dataset comprising 130 images recorded at 30 fps, resulting in a measurement time of 4.3 seconds per set. To address local pixel density variations due to inhomogeneous illumination, background images were generated by averaging 130 images per set and subtracted from each individual image. Figure 1 illustrates background-subtracted images taken at 0.5-second intervals.

Each image was first converted to grayscale and then to binary using the Otsu method [16] for automatic thresholding

to distinguish sperm cells from the background. The contours of sperm heads were identified using the Python OpenCV library, which implements border-following algorithms for the topological analysis of digitized binary images [17]. These algorithms determine the surroundness relations among the borders of a binary image and can be effectively used in component counting, shrinking, and topological structural analysis. The algorithms facilitated the accurate identification of sperm head contours by following the outermost borders, ensuring precise detection of the sperm cells. The center positions of the sperm heads were determined by averaging the x and y coordinates of the contours. Figure 2 illustrates the detected sperm cells, with their centers marked in blue and contours in red.

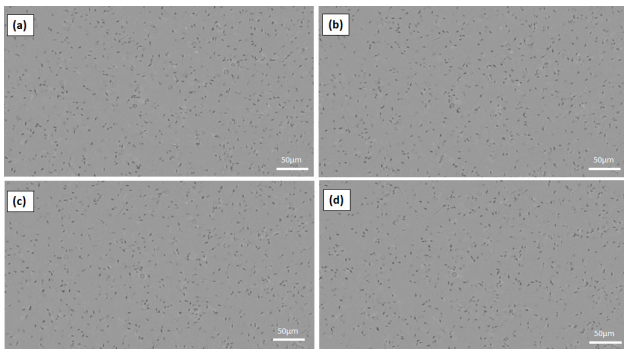


Figure 1 Background subtracted images taken at 0.5 second intervals at 10X magnification. (a) 0.5 sec, (b) 1.0 sec, (c) 1.5 sec, (d) 2.0 sec.

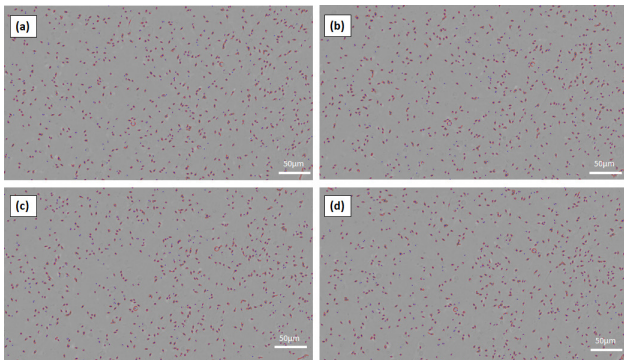


Figure 2 Sperms detected at 0.5 second intervals at 10X magnification. The centers of the sperms are shown as blue dots and the head region is shown as red lines. (a) 0.5 sec, (b) 1.0 sec, (c) 1.5 sec, (d) 2.0 sec.

Sperm traces in consecutive images were obtained by tracking center points assigned according to different acquisition times [15]. Figure 3 illustrates the tracking process on three consecutive images (j, j+1, j+2). At time j, the center position of a sperm cell is detected. This position is then compared with all sperm centers in the j+1 frame, and the closest match is recorded as the new center of that sperm in the j+1 image. This process is repeated for each sperm detected in the j image. Similarly, the process is carried out between images j+1 and j+2, and across other consecutive images to calculate the trajectory of each sperm head over time. In Figure 3,

the tracking process is depicted for sperm cells detected in equal numbers across consecutive images. However, if fewer sperm cells are detected in the subsequent image, it indicates that M sperm tracks were terminated in the previous image. Conversely, if more sperm cells are detected in the next image, it suggests that M new sperm tracks were initiated. Consequently, the initial and final frames of sperm traces may differ, leading to variations in track lengths among sperm.

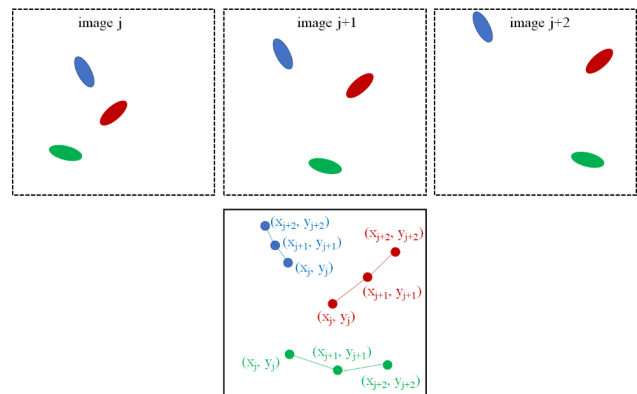


Figure 3 Sperm track illustration using sperm center points on 3 consecutive images.

In Figure 4, sperm tracks at different times are displayed in different colors, with traces of the same sperm coded with the same color. It is evident that some tracks continued across all images, while some traces were terminated, and new ones were created. For kinematic parameter measurements, only sperm tracks that were observed in at least 5 consecutive images were considered.

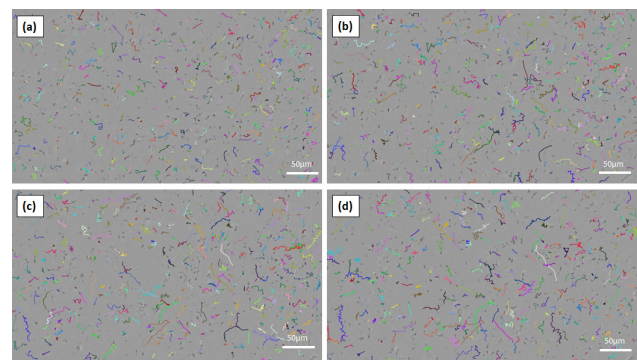


Figure 4 Tracks of sperms in different images at 10x magnification. Each sperm tracked is shown with a different color. (a) 0.5 sec, (b) 1.0 sec, (c) 1.5 sec, (d) 2.0 sec.

The metrics, developed in Python, measured six essential kinematic parameters [10]. The curvilinear velocity (VCL) of a sperm was calculated using the distance between center points of the cell in consecutive images. For instance, the VCL at position j, with coordinates (x_j, y_j) in image j and (x_{j+1}, y_{j+1}) in image j+1, is computed using Equation 1, where $\Delta t = 1/\text{fps}$ represents the time difference between consecutive images.

The linear velocity (VSL) was determined using the distance between the sperm's initial position (x_0, y_0) and final position (x_M, y_M) over time, as given by Equation 2. The average path velocity (VAP) was calculated using a moving average of the sperm's track with a value set to 5 frames (0.17 sec). For example, the VAP between averaged positions (x_j, y_j) in image j and (x_{j+1}, y_{j+1}) in image $j+1$ is given by Equation 3. The amplitude of lateral head (ALH) represents the amplitude difference between the VCL and VAP curves, with maximum and average ALH values calculated for each sperm. Beat cross frequency (BCF) was determined from the intersection points of the VCL and VAP curves, with the time difference between these points used in the analysis. The mean angular displacement (MAD) for each sperm in successive images was calculated using Equation 4. The VCL, VAP, BCF, and MAD values were computed for each sperm track, and their average values were recorded.

$$VCL_j = \frac{\sqrt{(x_{j+1} - x_j)^2 + (y_{j+1} - y_j)^2}}{\Delta t} \quad (1)$$

$$VSL = \frac{\sqrt{(x_M - x_0)^2 + (y_M - y_0)^2}}{\Delta t} \quad (2)$$

$$VAP_j = \frac{\sqrt{(x_{j+1} - x_j)^2 + (y_{j+1} - y_j)^2}}{\Delta t} \quad (3)$$

$$MAD_j = \cos^{-1} \left(\frac{x_j x_{j+1} + y_j y_{j+1}}{\sqrt{x_j^2 + y_j^2} \sqrt{x_{j+1}^2 + y_{j+1}^2}} \right) \quad (4)$$

Figure 5 shows examples of sperm tracks with different lengths in time. In the left column, black dots represent the positions of tracked sperm across different images, showing the VCL curve. The VAP curve, calculated by averaging VCL points, is shown with a red line. Blue dots indicate the starting and ending positions used for VSL analysis. In the right column, green dots mark the intersections of the VCL and VAP curves for BCF analysis, and the blue line indicates the maximum ALH distance between the VCL and VAP curves. These calculations were performed separately for each sperm track in four datasets.

The kinematic parameter LIN, which expresses the linearity of the curvilinear path, was determined by the percentage ratio of the mean VSL to VCL values. WOB, measuring the amount of wobbling in the sperm cell's movement path compared to the average path, was calculated by the ratio of VAP to VCL values. The STR parameter, reflecting the degree of straightness of the sperm's mean movement path, was calculated as the percentage ratio of VSL to VAP values. The motility parameter MOT was determined by the ratio of sperm with a mean VCL value greater than $5 \mu\text{m/s}$ to the total sperm count. The immobility parameter IM was calculated by the ratio of sperm with a velocity less than $5 \mu\text{m/s}$ to the total sperm count. Additionally, sperm with a VCL velocity greater than $25 \mu\text{m/s}$ were classified as progressive motility, while those with a velocity less than $25 \mu\text{m/s}$ were categorized

as non-progressive motility. The percentage of progressive sperm (PR) to total sperm count and the percentage of non-progressive sperm (NP) to total sperm count were calculated. Figure 6 summarizes the key stages in detecting and tracking sperm cells, from image acquisition to preprocessing, detection, tracking, and post-processing, highlighting the methods and techniques used at each step for precise analysis. Table 1 provides an overview of the parameters measured in the study, along with brief descriptions of each.

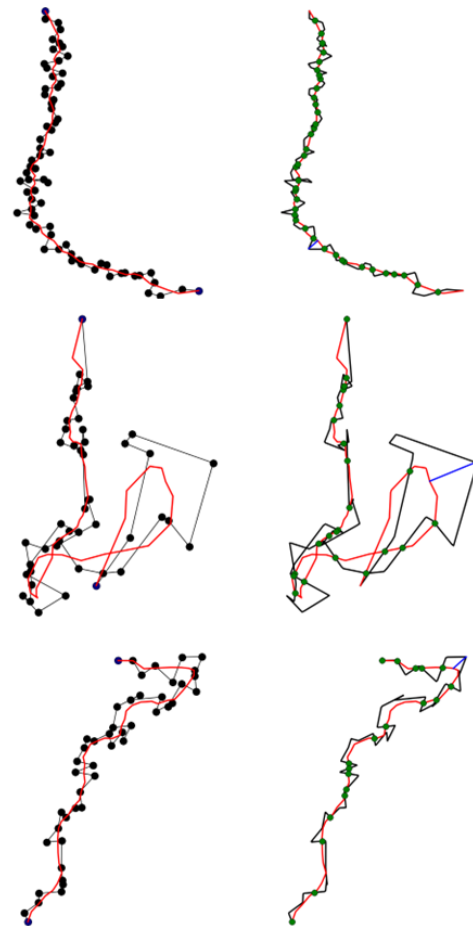


Figure 5 Examples of sperm tracks with different lengths.

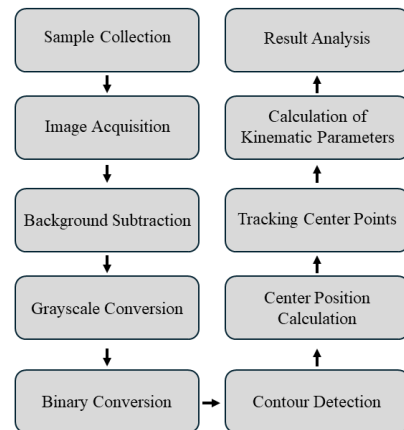


Figure 6 Workflow for detecting and tracking sperm cells.

Table 1 Summary of the parameters used in the study with brief descriptions.

Parameter	Description
VCL (Curvilinear Velocity)	Distance traveled by sperm between consecutive images.
VSL (Straight-Line Velocity)	Distance between the sperm's initial and final positions over time.
VAP (Average Path Velocity)	Moving average velocity along the sperm's track.
ALH (Amplitude of Lateral Head)	Amplitude difference between VCL and VAP curves.
BCF (Beat Cross Frequency)	Frequency of intersections between VCL and VAP curves.
MAD (Mean Angular Displacement)	Angular displacement of the sperm in successive images.
LIN (Linearity)	Ratio of VSL to VCL, indicating the straightness of the path.
WOB (Wobble)	Ratio of VAP to VCL, measuring the path wobble.
STR (Straightness)	Ratio of VSL to VAP, indicating the straightness of the average path.
MOT (Motility)	Ratio of sperm with VCL > 5 $\mu\text{m/s}$ to total sperm count.
IM (Immobility)	Ratio of sperm with VCL < 5 $\mu\text{m/s}$ to total sperm count.
PR (Progressive Motility)	Percentage of sperm with VCL > 25 $\mu\text{m/s}$.
NP (Non-Progressive Motility)	Percentage of sperm with VCL < 25 $\mu\text{m/s}$.

RESULTS AND DISCUSSION

Sperm count was calculated over approximately 4.3 seconds, with cells detected in 130 images per dataset. Figure 7(a) illustrates the variation in sperm count over time for the second dataset, demonstrating low variation around the mean value. Figure 7(b) shows the variation in sperm count per micrometer cubed over time, with red dashed lines indicating the mean value and green dashed lines representing WHO reference values. These analyses were repeated for each dataset, and the average sperm count, and sperm count per micrometer cubed were computed for four datasets captured three minutes apart. Table 2 presents the mean values for each dataset along with interquartile ranges (25th–75th percentile), indicating that 50% of the data falls within these ranges. The lowest average sperm count, and sperm count per cubic micrometer were 557 and 82.2×10^{-6} , respectively. The mean sperm count across all datasets was 609.1 ± 60.3 , and the sperm count per cubic micrometer was $89.9 \times 10^{-6} \pm 8.9 \times 10^{-6}$, which falls within the WHO reference values (15×10^6 – 259×10^6) [18].

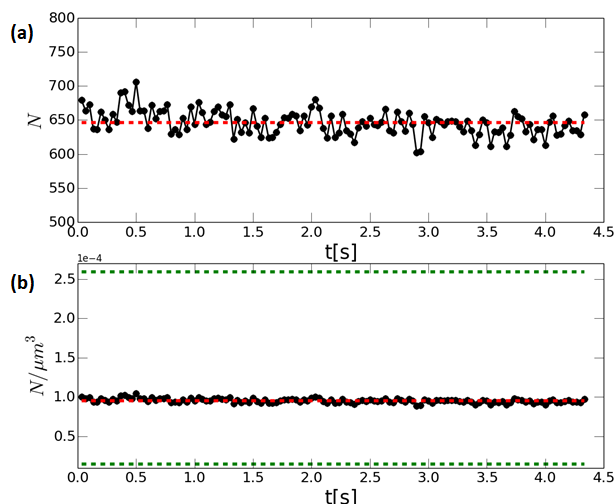


Figure 7 Average number of sperms in data set 2 and the number of sperms per micrometer cubed. The red dashed lines represent the mean value, and the green dashed lines represent the WHO reference limits.

Table 2 Average sperm count (N), and sperm count per cubic micrometer obtained in the four datasets. Values in parentheses indicate interquartile ranges (25th–75th percentile). The mean sperm count across all datasets is 609.1 (standard deviation 60.3), and the sperm count per cubic micrometer is 89.9×10^{-6} (standard deviation 8.9×10^{-6}).

DATA SET	N	$N/\mu\text{m}^3 \times 10^{-6}$
1	557.3 (547.0, 567.5)	82.2 (80.7, 83.8)
2	646.1 (634.5, 657.0)	95.4 (93.6, 97.0)
3	674.7 (662.5, 687.0)	99.6 (97.8, 101.4)
4	558.4 (535.5, 580.5)	82.4 (79.0, 85.7)

Table 3 presents the mean kinematic parameters obtained from all sperm in the four datasets. The total number of sperm tracked and analyzed ranged from 1178 to 1399. Values in parentheses represent interquartile ranges (25th and 75th percentiles). The VCL across all datasets was found to be greater than 70 $\mu\text{m/s}$, while the VAP and VSL values were greater than 45 $\mu\text{m/s}$ and 36 $\mu\text{m/s}$, respectively. As expected, VCL was greater than VAP, and VAP was greater than VSL. The average ALH was approximately 1 μm , with a maximum ALH around 3 μm . The BCF was approximately 15 Hz across all datasets. LIN was approximately 50% in all datasets, indicating sperm tracks were mostly straight. WOB was approximately 55% for all datasets, and STR values ranged from 63% to 75%. The motility (MOT) parameter was around 90%, indicating high sperm motility, while the immobility (IM) parameter was approximately 10%. Progressive motility (PR) was found to be 80%, and non-progressive motility (NP) was around 20%.

Table 3 Mean kinematic parameters for sperm from four datasets. Values in parentheses indicate interquartile ranges (25th-75th percentile).

DATASET	1	2	3	4
N	1254	1317	1399	1178
VCL [$\mu\text{m/s}$]	73.8 (46.0, 97.8)	72.7 (43.2, 97.8)	73.8 (47.5, 96.7)	76.3 (47.0, 103.2)
VAP [$\mu\text{m/s}$]	45.8 (26.2, 62.3)	45.6 (24.5, 63.5)	46.6 (27.0, 63.4)	49.5 (27.2, 68.3)
VSL [$\mu\text{m/s}$]	36.5 (16.5, 53.5)	36.1 (14.9, 53.5)	37.0 (16.3, 54.2)	40.4 (15.3, 60.2)
ALH max. [μm]	2.8 (1.6, 3.8)	2.9 (1.5, 3.8)	2.8 (1.7, 3.6)	2.8 (1.6, 3.8)
ALH mean [μm]	1.1 (0.6, 1.5)	1.0 (0.6, 1.4)	1.0 (0.6, 1.4)	1.0 (0.6, 1.4)
BCF [Hz]	15.2 (11.7, 18.4)	15.3 (12.0, 18.3)	15.3 (11.7, 18.5)	15.6 (12.5, 18.8)
MAD [$^\circ$]	30.2 (18.2, 39.0)	31.3 (18.4, 40.5)	31.0 (17.9, 39.7)	29.5 (17.5, 37.2)
LIN [%]	49.5	49.6	50.1	52.9
STR [%]	79.7	78.8	79.3	81.7
WOB [%]	62.1	63	63.2	64.8
MOT [%]	95.7	96.2	95.2	98.9
PR [%]	76.3	74.8	76.6	76.2
NP [%]	19.4	21.4	18.6	22.7
IM [%]	4.3	3.8	4.8	1.1

The mean kinematic parameters across all datasets are presented in Table 4. The standard deviation values indicate that the variation between datasets is low. It was estimated that $VCL = 1.58 \times VAP$ and $VAP = 1.25 \times VSL$, with VCL being approximately twice as great as VSL. This indicates that the wobbling is 63%, the straightness is 80%, and the linearity is around 50%. The maximum distance between the VCL and VAP curves is $2.8 \mu\text{m}$, while the average distance is $1 \mu\text{m}$. The BCF was approximately 15 Hz (fps/2), indicating that the VCL and VAP curves intersected every two frames. Additionally, sperm samples from Subject A, which exhibited high motility (96%), also showed a high progressive sperm count (76%).

Table 4 Mean and standard deviation of kinematic parameters from 4 data sets.

	MEAN	SD
VCL [$\mu\text{m/s}$]	74.2	1.5
VAP [$\mu\text{m/s}$]	46.9	1.8
VSL [$\mu\text{m/s}$]	37.5	2.0
ALH maks. [μm]	2.8	0.1
ALH ort. [μm]	1.0	0.1
BCF [Hz]	15.4	0.2
MAD [$^\circ$]	30.5	0.8
LIN [%]	50.5	1.6
STR [%]	79.9	1.3
WOB [%]	63.3	1.1
MOT [%]	96.5	1.7
PR [%]	76.0	0.8
NP [%]	24.0	0.8
IM [%]	3.5	1.7

Some of the measured parameters in this study were compared with those previously reported for human sperm in the literature. Notably, no study has been found that reports all 14 parameters simultaneously. Table 5 demonstrates that the VCL, VAP, VSL, ALH, and BCF values from this study fall within the ranges found in the literature. We emphasize methodological differences and performance metrics rather than direct comparisons, given that the datasets are not identical.

Table 5 Comparison of some of the kinematic parameters measured in the study with values found in the literature.

	VCL	VAP	VSL	ALH max.	ALH mean	BCF
Current Study	74.2	46.9	37.5	2.8	1.0	15.4
Sloter et al. [14]	80.7	55.8	49.1	3.7	-	25.2
Kraemer et al. [19]	119	-	54	7.5	-	-
Di Caprio et al. [9]	69.5	67.7	22.4	-	-	-
Hirano et al. [20]	82.5	46.1	56.1	4	-	23.6
Akashi et al. [21]	57.4	-	-	-	1.4	10
Mortimer et al. [22]	83.5	-	-	3.8	2.4	-
Davis et al. [23]	52	-	32.3	2.99	-	-

CONCLUSION

This study introduces a novel CASA system capable of quantitatively evaluating human sperm kinematic parameters through digital image processing. The system's performance was validated against WHO reference values, demonstrating its potential for clinical application in male infertility diagnostics. Continued development and optimization of the system will further enhance its utility in reproductive health assessments.

The kinematic parameters reported in this study may provide quantitative evaluations for male infertility, although no definitive conclusions can be drawn about human infertility. It is also believed that the current system will contribute to the literature by examining parameters that affect reproduction positively or negatively. In such studies, the number and motility of human sperm, directly impacting infertility, would be more accurately studied, allowing for comprehensive evaluation of the CASA method as a reliable diagnostic tool. Additionally, this technique could enable the diagnosis of specific diseases based solely on sperm kinematics in future disease-based studies. Future work will focus on enhancing the algorithms for real-time analysis and incorporating additional parameters for a comprehensive assessment of sperm quality.

Acknowledgement

The authors wish to thank Prof. Dr. Öner Odabaş for his assistance in patient sample collection and ethical approval.

References

- Erdemir F, Firat F, Gençten Y. The evaluation and clinical significance of sperm morphology. *Turk Urol Sem.* 2011 Jan;2:11-7.
- Cui W. Mother or nothing: the agony of infertility. *World Health Organization. Bulletin of the World Health Organization.* 2010 Dec 1;88(12):881.
- Gökçe A. Standard Semen Analysis Criteria of World Health Organization. *Turk Urol Sem.* 2011 Jan;2:1-7.
- Amann RP, Katz DF. Andrology lab corner*: Reflections on casa after 25 years. *Journal of andrology.* 2004 May 6;25(3):317-25.
- Katz DF, Davis RO, Delandmeter BA, Overstreet JW. Real-time analysis of sperm motion using automatic video image digitization. *Computer methods and programs in biomedicine.* 1985 Dec 1;21(3):173-82.
- Abbiramy VS, Shanthi V, Allidurai C. Spermatozoa detection, counting and tracking in video streams to detect asthenozoospermia. In 2010 International Conference on Signal and Image Processing 2010 Dec 15 (pp. 265-270). IEEE.
- Leung C, Lu Z, Esfandiari N, Casper RF, Sun Y. Detection and tracking of low contrast human sperm tail. In 2010 IEEE International Conference on Automation Science and Engineering 2010 Aug 21 (pp. 263-268). IEEE.
- Ravanfar MR, Moradi MH. Low contrast sperm detection and tracking by watershed algorithm and particle filter. In 2011 18th Iranian Conference of Biomedical Engineering (ICBME) 2011 Dec 14 (pp. 260-263). IEEE.
- Di Caprio G, El Mallahi A, Ferraro P, Dale R, Coppola G, Dale B, Coppola G, Dubois F. 4D tracking of clinical seminal samples for quantitative characterization of motility parameters. *Biomedical optics express.* 2014 Mar 1;5(3):690-700.
- Elsayed M, El-Sherry TM, Abdelgawad M. Development of computer-assisted sperm analysis plugin for analyzing sperm motion in microfluidic environments using Image-J. *Theriogenology.* 2015 Nov 1;84(8):1367-77.
- Urbano LF, Masson P, VerMilyea M, Kam M. Automatic tracking and motility analysis of human sperm in time-lapse images. *IEEE transactions on medical imaging.* 2016 Nov 18;36(3):792-801.
- Boumaza K, Loukil A. Computer-Assisted Analysis of Human Semen Concentration and Motility. *International Journal of E-Health and Medical Communications (IJEHMC).* 2020 Oct 1;11(4):17-33.
- Hernández-Ferrándiz D, Pantrigo JJ, Cabido R. SCASA: From synthetic to real computer-aided sperm analysis. In *International Work-Conference on the Interplay Between Natural and Artificial Computation 2022 May 24* (pp. 233-242). Cham: Springer International Publishing.
- Sloter E, Schmid TE, Marchetti F, Eskenazi B, Nath J, Wyrobek AJ. Quantitative effects of male age on sperm motion. *Human Reproduction.* 2006 Nov 1;21(11):2868-75.
- Chenouard N, Smal I, De Chaumont F, Maška M, Sbalzarini IF, Gong Y, Cardinale J, Carthel C, Coraluppi S, Winter M, Cohen AR. Objective comparison of particle tracking methods. *Nature methods.* 2014 Mar;11(3):281-9.
- Yousefi J. Image binarization using Otsu thresholding algorithm. Ontario, Canada: University of Guelph. 2011 Apr 18;10.
- Suzuki S. Topological structural analysis of digitized binary images by border following. *Computer vision, graphics, and image processing.* 1985 Apr 1;30(1):32-46.
- World Health Organization. WHO laboratory manual for the examination and processing of human semen. World Health Organization; 2010.
- Kraemer M, Fillion C, Martin-Pont B, Auger J. Factors influencing human sperm kinematic measurements by the Celltrak computer-assisted sperm analysis system. *Human reproduction (Oxford, England).* 1998 Mar 1;13(3):611-9.
- Hirano Y, Shibahara H, Shimada K, Yamanaka S, Suzuki T, Takamizawa S, Motoyama M, Suzuki M. Accuracy of sperm velocity assessment using the Sperm Quality Analyzer V. *Reproductive medicine and biology.* 2003 Dec;2:151-7.
- Akashi T, Watanabe A, Komiya A, Fuse H. Evaluation of the sperm motility analyzer system (SMAS) for the assessment of sperm quality in infertile men. *Systems biology in reproductive medicine.* 2010 Dec 1;56(6):473-7.
- Mortimer ST, Swan MA. Variable kinematics of capacitating human spermatozoa. *Human reproduction.* 1995 Dec 1;10(12):3178-82.
- Davis RO, Katz DF. Standardization and comparability of CASA instruments. *Journal of Andrology.* 1992 Jan 2;13(1):81-6.